Delocalization of the multifunctional RNA splicing factor TLS/FUS in hippocampal neurones: exclusion from the nucleus and accumulation in dendritic granules and spine heads.

Agnès Belly [1], Françoise Moreau-Gachelin [2], Rémy Sadoul [1], Yves Goldberg [1, 3, 4]

(1) Laboratoire Neurodégénérescence et Plasticité, Université Joseph Fourier and INSERM EMI 0108, Pavillon de Neurologie, Centre Hospitalier Universitaire, F-38043 Grenoble cedex 9, France

(2) Laboratoire de Transduction du Signal et Oncogenèse, Institut Curie and Inserm U528, 26 rue d'Ulm, 75 248 Paris cedex 05, France

(3) Département de Réponse et Dynamique Cellulaires, CEA Grenoble, F-38054 Grenoble cedex 9, France

(4) Corresponding author

E-mail : yves.goldberg@ujf-grenoble.fr

Phone: +33 476 76 88 81

Fax: +33 476 76 58 22

Postal address: see (1)

20 pages, 3 figures

Abstract

Long-term synaptic change in the cortex and the hippocampus is believed to require the highly localized delivery and translation of mRNAs in the dendritic shafts and spines. The molecular interactions that underlie local signalling between synapses and mRNAs are still largely undefined. After purification from total brain extracts, the NMDA receptor is known to be associated with numerous proteins, including the multifunctional RNA-binding factor TLS (also called FUS). In non-neural tissue, TLS is a vital nuclear protein with roles in DNA repair, homologous recombination, transcriptional regulation and pre-mRNA processing. We have examined the distribution of TLS in hippocampal neurones, both in the adult brain and in mature primary cultures, using subcellular fractionation and immunofluorescence techniques. TLS is largely excluded from the neuronal nucleus and is found in the cytosol and in somatodendritic particles. In some of these particles, TLS colocalizes with Sam68, a nuclear RNA-binding protein that we previously showed is incorporated into dendritic RNA granules. Some of the TLS clusters also colocalize with NMDA receptor clusters. Finally, TLS clusters are occasionally seen within spine heads. The apparent removal of TLS from the nucleus might result in specific patterns of mRNA transcription or splicing in hippocampal neurones. TLS may thus also contribute to steering, anchoring or regulating mRNAs at synaptic sites.

Introduction

The development and plasticity of synapses depend in part on protein synthesis taking place in the dendrites [16]. Polyribosomes are often docked at the basis of dendritic spines, and transferred into spine heads following long-term potentiation. It is largely unknown how such a synapse-specific regulation of mRNAs is achieved.

In cultured neurones, dendritic mRNAs such as *CaMKIIα* and *Arc* are packaged in clusters, termed "RNA granules", that move along the dendrites and sometimes locate close to synapses [15]. A growing number of RNA-binding proteins have been found to colocalize with RNA granules *in situ*, or to copurify with biochemically isolated granule preparations. A few of these proteins, including ZBP1 and FMRP, were shown to enter (and exit) spine heads [1]. A range of RNA-associated proteins, including translation factors and some RNA granule proteins, have also been identified in highly purified postsynaptic density preparations, consistent with synaptic localization of ribonucleoproteic complexes [13]. The molecular interactions responsible for retaining such complexes in the spine are undefined; they may involve anchoring of RNA-associated proteins to postsynaptic density proteins.

A few years ago, in a large-scale analysis of proteins that copurified with NMDA receptor from mouse brain extracts, the RNA-binding protein TLS (also called FUS) was found to exist in the receptor complex [9]. TLS (Translocated in Liposarcoma) has so far been known for its manifold functions in nuclear processes, including DNA transcription, pre-mRNA processing, homologous recombination, and DNA repair. The biological importance of the protein is underscored by the rapid postnatal death of TLS-deficient mice [8] and by the primary role of TLS or TLS-derived gene fusions in the evolution of specific tumours [14]. TLS interacts with general and promoter-specific transcription factors and with elements of the splicing machinery [6 , 10]. Consistent with its known function, in proliferating cells, TLS is concentrated in specific regions of the cell nucleus; however, TLS is capable of shuttling

between nucleus and cytoplasm, a minor fraction of TLS molecules being associated with cytoplasmic mRNAs [17].

The identification of TLS as a (direct or indirect) partner of the NMDA receptor raises the possibility that this protein might participate in the docking and/or regulation of mRNAs at excitatory synaptic sites. However, it has not yet been established whether the ordinarily nuclear TLS can be detectably localized at synaptic or dendritic sites, and whether the protein colocalizes with NMDA receptor clusters in defined regions of the brain. This question is addressed here.

Materials and Methods

Antibodies and plasmid

The anti-TLS rabbit antiserum has been described [6]; this antibody does not cross-react with the TLS-related protein EWS (unpublished data). Affinity-purified anti-TLS IgG (used in all experiments) was purified from the antiserum as described [7], using beads that had been coupled to a GST-TLS fusion protein [6]; the antibody was further depleted of any anti-GST components by adsorption to unfused GST. The anti-Sam68 monoclonal antibody was derived from either clone 7-1 (Santa Cruz, Inc), or clone P20120 (BD Transduction). The monoclonal antibody raised against the myc epitope (clone 9E10) was obtained from Santa Cruz, Inc. Horseradish peroxidase (HRP)-conjugated protein A was obtained from BD Transduction. HRP-conjugated goat anti-mouse antibody was purchased from Jackson Laboratories. Fluorescent conjugates were purchased from Molecular Probes. The myc-TLS plasmid (pcs3-mt-TLS) [6]allows expression of full-length TLS fused in-frame with a hexamer of the myc epitope at the N terminus.

Fractionation of hippocampal tissue

All procedures using animals conformed to institutional guidelines, in compliance with European Community Council Directive 86/609. Hippocampi were dissected from adult (200-210 g) male OFA rats (Charles Rivers, Lyon, France), and subjected to subcellular fractionation essentially as described by Feng et al. [4]. The hippocampi were manually ground in a Potter homogenizer with a Teflon pestle (0.15 mm clearance, 15 strokes), in 1 ml ice-cold H buffer (4mM Hepes-NaOH, pH 7.4, 0.32 M sucrose, 1 mM $MgCl_2$, 1 mM sodium orthovanadate, 1 mM dithiothreitol, 100 nM microcystine-LR (Sigma), protease inhibitors (EDTA-free "Complete", Roche Molecular). The homogenate was filtered through a 100 μm-mesh nylon filter (Millipore) and centrifuged at 800 x g for 10 min. at 4°C. The resulting S1 supernatant was centrifuged at 9500 x g for 20 min. at 4°C. The S2 supernatant was

centrifuged at 130,000 x g for 1 hr at 4°C. For all fractions, total protein concentration was measured and samples were boiled for 5 min. in Laemmli gel buffer. Equal protein amounts of the samples were resolved on a 8% polyacrylamide-SDS gel and transferred onto a PVDF membrane (Millipore). The membrane was probed with anti-TLS antibody (200 ng/ml) or anti-Sam68 antibody (200 ng/ml), and after incubation with HRP-conjugated secondary reagents, bands were revealed by chemiluminescence (Super-Signal Pico, Pierce). Photographs of the blots were digitized with a flatbed scanner. Care was taken to ensure signal linearity.

Immunostaining of brain tissue

Vibratome sections (30 μm thick) of PFA-fixed adult rat hippocampus were prepared as previously described [5]. For staining, the sections were incubated at 4°C for 20 min in cold (-20°C) ethanol; rinsed with TBS (20 mM Tris-HCl, pH 7.4, 150 mM NaCl); preincubated for 30 min at room temperature in blocking buffer (TBS containing 3% goat serum and 0.1% Triton X-100); and incubated with primary antibodies (2 μg/ml) in blocking buffer for 48 hr at 4°C. Sections were then washed (3x10 min in TBS containing 0.1% Triton X-100); incubated for 1 hr at R.T. with blocking buffer containing Alexa 488-conjugated goat anti-rabbit IgG and Alexa 594-conjugated goat anti-mouse IgG; washed as above; rinsed in water, and mounted on slides in Mowiol medium.

Immunostaining of cultured neurones

Hippocampal neuronal cultures were prepared from E19 rat embryos (Charles Rivers) essentially as described by Banker and Goslin [2] with a few modifications. After dissecting, trypsinizing and triturating the hippocampi, hippocampal neurones were resuspended in Dulbecco's minimal essential medium containing glutamine, penicilline, streptomycine, and 10% heat-inactivated horse serum (Invitrogen), and plated at a density of 0.5 -1 x 10^4 per cm^2 on 13 mm glass coverslips (Marienfeld, Germany) coated with poly-L-lysine (Sigma).

Supporting high-density cultures were prepared by seeding in the same medium 1.5 x 10^5 hippocampal cells per well in 24-well plates (Becton-Dickinson) in which small pegs had been formed at the bottom of the wells, by brief contact with a soldering iron. After 3-4 hours, the medium of the wells was changed to Neurobasal (Invitrogen) containing antibiotics, glutamine, sodium pyruvate and B27 supplement (Invitrogen). The coverslips were transferred into the wells, with attached neurones facing downward. The cultures were fed once a week with 1:3 volume of fresh medium. After 4 weeks, neurones were fixed for 20 min. at R.T. in PBS containing 4% paraformaldehyde and 4% sucrose; washed with PBS; permeabilized for 10 min. at 4°C with 0.1% Triton X-100 in PBS; preincubated for 1 hr in PBS containing 3% bovine serum albumin (BSA); and stained for 1 hr in PBS containing 3% BSA and 2 µg/ml primary antibodies. After rinsing in PBS, fluorescent conjugates were applied for 1 hr (Alexa 488-conjugated anti-rabbit IgG, rhodamine-conjugated phalloidin, and (for triple labelling) Alexa 350-conjugated anti-mouse IgG in PBS/ 3% BSA). Coverslips were rinsed 3 times in PBS, 3 times in water, and mounted on slides in Mowiol medium.

Microscopy

Images of the brain sections and of doubly stained neurones were acquired as z-stacks of 512 x 512 pixel frames with a Zeiss LSM 510 laser scanning confocal microscope, using a 63X (1.4 NA) objective. For dual colour imaging, care was taken to exclude contamination between channels, and to maximize the dynamic range at both wavelengths. Images of triply stained neurones were acquired as 1300 x 1030 pixel frames with a Zeiss Axiovert 200 microscope, using a 100x (1.4 NA) objective, appropriate bandpass filters (Chroma Technologies) and a cooled CCD camera (Micromax, Roper Scientific). Again, care was to taken to maximize the dynamic range of all channels. Image files were processed with Metamorph (Universal Imaging) and Photoshop (Adobe). Non-specific background fluorescence, estimated as at most (mean+2SD) of pixels in an empty region, was subtracted

from the raw images; the resulting images were contrasted to highlight the somatodendritic granules. To establish the specificity of TLS labelling, images of specifically stained and control sections were acquired under identical illumination and scanning conditions, and the average fluorescence of the control section was used as background value for both images.

Culture, transfection and staining of HEK-293 cells

HEK-293 cells were maintained in DMEM supplemented with 10% fetal calf serum (Invitrogen). The cells were seeded on glass coverslips kept in a 6-cm dish, and transfected the next day with 5 µg myc-TLS plasmid using Fugene reagent (Roche Molecular). 48 hr later cells were fixed in PBS containing 4% paraformaldehyde for 20 min. at R.T., and subjected to immunofluorescent staining essentially as described for neurones, using 2 µg/ml anti-TLS antibody and 200 ng/ml anti-myc monoclonal antibody.

Results

Adult hippocampal tissue was fractionated into nuclear, membrane and cytosolic fractions, and the relative abundance of the TLS protein was determined by Western immunoblotting of the various fractions. Unlike the case in proliferating cell types, TLS was nearly absent from the nuclei (Fig.1A, upper panel, lane 2). The 75 kD band expected for TLS (arrow) was enriched in the soluble fraction (lane 6). Some of the 75 kD protein could also be recovered together with microsomal membranes and polysomes in the P3 pellet (lane 5).

As a control for the integrity of the various fractions, the blot was reprobed with an antibody raised against Sam68, an RNA-binding protein of a different type. Consistent with known results [5], Sam68 was most abundant in the nuclear fraction (lower panel). Thus, the absence of nuclear TLS did not arise from mere breakdown of the nuclei. This result suggests that in hippocampal tissue, most of the TLS protein resides in the cytoplasmic compartment, with a minor but definite fraction associated with the polysomal fraction.

In addition, an immunoreactive band of 100 kD was reproducibly detected, and enriched in the P2 and P3 fractions (arrowhead). Whether this band arises from antibody cross-reactivity or represents some modified form of the TLS protein is not known at present.

To define the subcellular localization of the TLS protein in more detail, immunofluorescent detection was performed. The specificity of our anti-TLS antibody in immunofluorescence assays was first verified in cultured HEK293 cells that had been transfected with a myc-TLS construct. The myc-tagged protein was detected by dual staining with anti-myc monoclonal antibody and anti-TLS antibody. In cells expressing the construct, the anti-TLS antibody generated intense nuclear staining that exactly overlapped with the distribution of the myc-tagged protein (Fig. 2A). In addition, in cells that had failed to take up the myc-TLS plasmid, the anti-TLS antibody revealed an identical but much fainter pattern of nuclear staining, corresponding to the usual distribution of the endogenous TLS protein in proliferating cells

(Fig. 2B, arrow). Thus, the anti-TLS antibody used in this study is capable of specifically staining the *bona fide* TLS protein. No staining was obtained with preimmune IgG (not shown).

The distribution of TLS staining in sections of adult hippocampus was then examined by confocal microscopy and compared to that of two reference proteins, i.e. the predominantly nuclear RNA-binding protein Sam68, and the NR1 subunit of the NMDA receptor. TLS staining was detected in the cell bodies and throughout the dendritic layers (stratum moleculare, stratum radiatum), but was largely excluded from the neuronal nuclei (Fig. 2C). In contrast, the pattern of Sam68 staining was predominantly nuclear and perinuclear, with a low level of dendritic fluorescence, in agreement with our previous results (Fig. 2D). Higher magnification views indicated that the TLS immunofluorescence displayed both a granular component and a diffuse component. This pattern agrees well with the distribution found by biochemical analysis. Individual TLS clusters could be visualized in the perinuclear region of dentate granule neurones (Fig. 2F) and in the perikaryon and dendritic trunk of CA1 pyramidal neurones (Fig. 2I). Despite the overall clearly distinct distribution of the two proteins, some of the TLS clusters overlapped with somatodendritic Sam68 granules (arrows in Figs. 2F-H, I-K). Because Sam68 granules have been shown to associate with RNA [3], this suggests that these TLS/Sam68 clusters correspond to RNA granules (see Discussion). Dual immunolabelling also indicated that some of the TLS clusters colocalized with NR1 clusters (Fig. 2L-N, arrows), suggesting that TLS may locate close to glutamatergic synapses.

To examine more closely the intra-dendritic localization of TLS, we used mature (4 week-old) cultures of hippocampal neurones. The dendritic accumulation of TLS was confirmed in triply stained neurones such as that of of Fig. 3A-D, in which TLS was labelled together with MAP2 (as a marker for dendritic trunks) and phalloidin (to highlight the F-actin-rich dendritic spines). Higher magnification view of the dendrites again showed that TLS condensed in

granules in the midst of diffuse staining (Fig. 3E). Of note, TLS granules were repeatedly found at the tip of dendritic spines (arrows in Fig. 3E and F), clearly outside of the dendritic trunk. These results were again confirmed by confocal microscopy. TLS was largely absent from the nucleus (Fig. 3, I-K). Instead, TLS clusters were found in the cell body and along the entire length of the dendrites (Fig. 3, L-N).

Discussion

The recent finding that TLS copurifies with the NMDA receptor complex [9] raises the intriguing possibility that both proteins may interact at the synapse. To our surprise, TLS was largely excluded from the nuclei of hippocampal neurones, in adult hippocampus *in situ* as well as in mature neuronal cultures. This suggests massive nuclear export of the protein. Alternatively, it is possible that TLS undergoes localized degradation in the nucleus. Indeed, compared to its abundance in other tissues, TLS is relatively scarce in the brain [12]. Whatever its mechanism, the depletion of nuclear TLS may conceivably play a role in neurone-specific transcription or splicing events. In cultured cell lines, increasing the intranuclear concentration of TLS has been shown either to inhibit or to potentiate the activity of specific transcription factors, and to bias exon selection in transcripts encoded by a transfected minigene [6]. Whether the lack of nuclear TLS may affect the sensitivity of neurones to DNA breaks, e.g. by ionizing radiation [8], is an open question.

Biochemical analysis indicated that in the cytoplasm, TLS was partitioned into a cytosolic pool and a particulate pool, sedimenting with the polysomal fraction. Diffuse and granular pools of TLS were also observed by immunofluorescence in the somatodendritic domain. The dendritic puncta often contained Sam68, an RNA-binding protein which, outside of the nucleus, becomes incorporated in RNA-containing dendritic granules [3, 5]. These observations suggest that some of the observed TLS clusters are in fact RNA granules, involved in dendritic mRNA transport or translation. It is possible that part of the punctuate immunofluorescence in fact arose from reaction of the antibody with the 100 kD protein seen in the polysomal fraction. Whether this band represents a modified, granule-specific form of TLS, or an antigenically related protein remains to be determined. However, the presence of *bona fide* TLS in dendritic granules is supported by several lines of evidence. A small but significant fraction of the 75 kD TLS protein was found in the polysomal pellet. Furthermore,

when transiently expressed in hippocampal neurones, myc-tagged TLS also clustered into dendritic puncta (unpublished data). Finally, a recent proteomic study identified TLS as one of the multiple RNA-binding proteins found in biochemically purified RNA transport granules [11]. Our data provide a morphological correlate to this biochemical result. The microscopically defined granules correspond to very large supramolecular complexes, in which mRNAs, ribosomes, motor proteins, and multiple RNA-binding proteins are associated [11]. TLS might possibly become recruited from the cytosolic TLS pool during the cytoplasmic maturation of these complexes.

In adult hippocampus, a subset of TLS puncta also colocalized with NMDA receptor clusters; furthermore, in cultured neurones, TLS puncta could be seen within spine heads. Thus, the biochemical association of TLS to NMDA receptors likely occurs in the spines. Our data suggest that TLS is in an ideal position to regulate mRNA docking or translation at excitatory post-synaptic sites, as a function of the local activity history. It will be important to determine the extent and functional effect of TLS association with mRNA in the dendrites and in the spines.

References

1   Antar, L.N., Afroz, R., Dictenberg, J.B., Carroll, R.C. and Bassell, G.J., Metabotropic Glutamate Receptor Activation Regulates Fragile X Mental Retardation Protein and Fmr1 mRNA Localization Differentially in Dendrites and at Synapses, J. Neurosci., 24 (2004) 2648-2655.

2   Banker, G., Asmussen, H. and Goslin, K., Rat Hippocampal Neurons in Low-Density Culture,2nd edn., MIT Press, 1998, 666 pp.

3   Ben Fredj, N., Grange, J., Sadoul, R., Richard, S., Goldberg, Y. and Boyer, V., Depolarization-induced translocation of the RNA-binding protein Sam68 to the dendrites of hippocampal neurons, J Cell Sci, 117 (2004) 1079-90.

4   Feng, Y., Gutekunst, C.-A., Eberhart, D.E., Yi, H., Warren, S.T. and Hersch, S.M., Fragile X Mental Retardation Protein: Nucleocytoplasmic Shuttling and Association with Somatodendritic Ribosomes, J. Neurosci., 17 (1997) 1539-1547.

5   Grange, J., Boyer, V., Fabian-Fine, R., Fredj, N.B., Sadoul, R. and Goldberg, Y., Somatodendritic localization and mRNA association of the splicing regulatory protein Sam68 in the hippocampus and cortex, J Neurosci Res, 75 (2004) 654-66.

6   Hallier, M., Lerga, A., Barnache, S., Tavitian, A. and Moreau-Gachelin, F., The Transcription Factor Spi-1/PU.1 Interacts with the Potential Splicing Factor TLS, J. Biol. Chem., 273 (1998) 4838-4842.

7   Harlow, E. and Lane, D., Using Antibodies: A laboratory Manual,2nd edn., Cold Spring Harbor Laboratory Press, 1999, 495 pp.

8   Hicks, G.G., Singh, N., Nashabi, A., Mai, S., Bozek, G., Klewes, L., Arapovic, D., White, E.K., Koury, M.J., Oltz, E.M., Van Kaer, L. and Ruley, H.E., Fus deficiency in mice results in defective B-lymphocyte development and activation, high levels of chromosomal instability and perinatal death, Nat Genet, 24 (2000) 175-9.

9   Husi, H., Ward, M.A., Choudhary, J.S., Blackstock, W.P. and Grant, S.G., Proteomic analysis of NMDA receptor-adhesion protein signaling complexes, Nat Neurosci, 3 (2000) 661-9.

10   Kameoka, S., Duque, P. and Konarska, M.M., p54nrb associates with the 5' splice site within large transcription/splicing complexes, EMBO J., 23 (2004) 1782-1791.

11   Kanai, Y., Dohmae, N. and Hirokawa, N., Kinesin Transports RNA: Isolation and Characterization of an RNA-Transporting Granule, Neuron, 43 (2004) 513-525.

12   Melot, T., Dauphinot, L., Sevenet, N., Radvanyi, F. and Delattre, O., Characterization of a new brain-specific isoform of the EWS oncoprotein, Eur J Biochem, 268 (2001) 3483-3489.

13   Peng, J., Kim, M.J., Cheng, D., Duong, D.M., Gygi, S.P. and Sheng, M., Semi-quantitative proteomic analysis of rat forebrain postsynaptic density fractions by mass spectrometry, J. Biol. Chem. (2004) M400103200.

14   Perrotti, D., Bonatti, S., Trotta, R., Martinez, R., Skorski, T., Salomoni, P., Grassilli, E., Iozzo, R.V., Cooper, D.R. and Calabretta, B., TLS/FUS, a pro-oncogene involved in multiple chromosomal translocations, is a novel regulator of BCR/ABL-mediated leukemogenesis, EMBO J., 17 (1998) 4442-4455.

15   Rook, M.S., Lu, M. and Kosik, K.S., CaMKIIalpha 3' Untranslated Region-Directed mRNA Translocation in Living Neurons: Visualization by GFP Linkage, J. Neurosci., 20 (2000) 6385-6393.

16   Steward, O. and Schuman, E.M., Compartmentalized synthesis and degradation of proteins in neurons, Neuron, 40 (2003) 347-59.

17   Zinszner, H., Sok, J., Immanuel, D., Yin, Y. and Ron, D., TLS (FUS) binds RNA in vivo and engages in nucleo-cytoplasmic shuttling, J Cell Sci, 110 (1997) 1741-1750.

Figure legends

Fig. 1: TLS is a predominantly cytoplasmic protein in hippocampal tissue. *A*. Fractionation scheme (see [4]). Total hippocampal homogenate (Hmg) was fractionated by successive centrifugation steps to yield the indicated pellets (P) and supernatants (S). Major components of each subcellular fraction are indicated. Note that the heavy membranes (P2) include intact synaptoneurosomes and mitochondria; the polysomal pellet also contains light (internal) membranes. *B*. Equal protein amounts (30 μg) of each subcellular fraction were loaded onto an SDS gel and analyzed by immunoblotting with antibody against TLS (top) or Sam68 (bottom). Arrow: TLS protein. Arrowhead: 100 kD protein of unknown identity.

Fig. 2: TLS localization in the hippocampus. *A*, *B*: specificity of the TLS antibody. HEK-293 cells transiently expressing myc-tagged TLS were doubly stained with anti-myc monoclonal antibody (*A*) and anti-TLS antibody (*B*). Labelling was visualized by wide-field fluorescence microscopy. Scale bar: 40 μm. Arrow: nuclear staining of endogenous TLS in a non-transfected cell. *C-N*: Coronal sections of adult hippocampus were doubly stained with anti-TLS antibody (*C,F,I, L*; green in *E, H, K, N*) and either anti-Sam68 monoclonal antibody (*D, G, J*; red in *E, H, K*) or anti-NR1 monoclonal antibody (*M*; red in *N*). Labelling was visualized by laser scanning confocal microscopy; shown are single confocal planes extracted from the middle of z series. *C-E*: granule cells and neuropil of the dorsal dentate gyrus. s.mo., stratum moleculare. Scale bar: 40 μm. *F-H*: granule cell layer of the dorsal dentate gyrus. Arrows: perikaryal TLS puncta that colocalize with Sam68 puncta. Scale bar: 10 μm. *I-K*: Pyramidal neurone in the CA1 layer. Arrows: TLS puncta that colocalize with Sam68 puncta in proximal dendrite. n, nucleus. Scale bar: 6.65 μm. *L-N*: CA1 neurones. In order specifically to evaluate the overlap of fluorescent puncta, images (acquired as in *C-K*) were thresholded so that the diffuse component of TLS fluorescence does not appear. Arrows: TLS puncta that

coincide with NR1 puncta. Scale bar: 10 μm. *O, P*: sections were immunostained after preincubation of the anti-TLS antibody with either unfused GST or GST-TLS fusion protein, and visualized by confocal microscopy under identical conditions. Scale bar: 40 μm.

Fig. 3: TLS exists in dendritic granules, some of which are localized within spines. *A-H*: fetal hippocampal neurones were allowed to mature in culture for 4 weeks, and then triply stained with anti-TLS antibody (*A*, *E*; green in *D*, *H*), rhodamin-conjugated phalloidin (*B*, *F*; red in *D*, *H*), and anti-MAP2 monoclonal antibody (*C*, *G*; blue in *D*, *H*). *A-D*: wide-field view of an isolated neurone; *E-H*: details of a dendrite. Arrows: TLS clusters (*E*) located outside of the dendritic trunk, overlapping with dendritic spine heads (*F*). Scale bar: *A-D*: 20 μm, *E-H*: 10 μm. *I-N*: cultured neurone, doubly stained with anti-TLS antibody (*I*, *L*, green in *K*, *N*) and rhodamin-conjugated phalloidin (*J*, *M*, red in *K*, *N*), and visualized by confocal microscopy. Single optical sections are shown to illustrate the distribution of labelling through the nucleus and soma (*I-K*) and the dendrites (*L-N*). Scale bar: 20 μm.

A

Hmg

800 g, 10 min

S1   **P1 (nuclei)**

9 500 g, 15 min

S2   **P2 (heavy mbr.)**

130 000 g, 60 min

S3 (cytosol)   **P3 (polysomes)**

B

	Hmg	P1	P2	S2	P3	S3
	1	2	3	4	5	6

Mr (kDa)

97

66

WB: TLS

| 1 | 2 | 3 | 4 | 5 | 6 |

97

66

WB: Sam68

Belly et al., Fig. 1
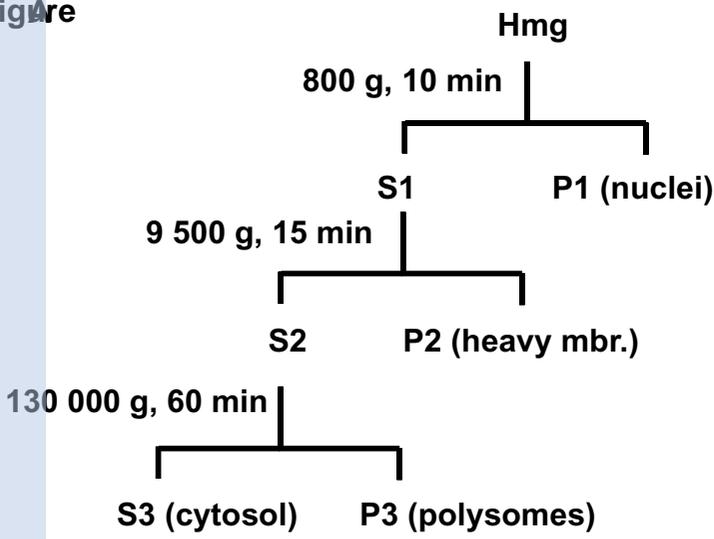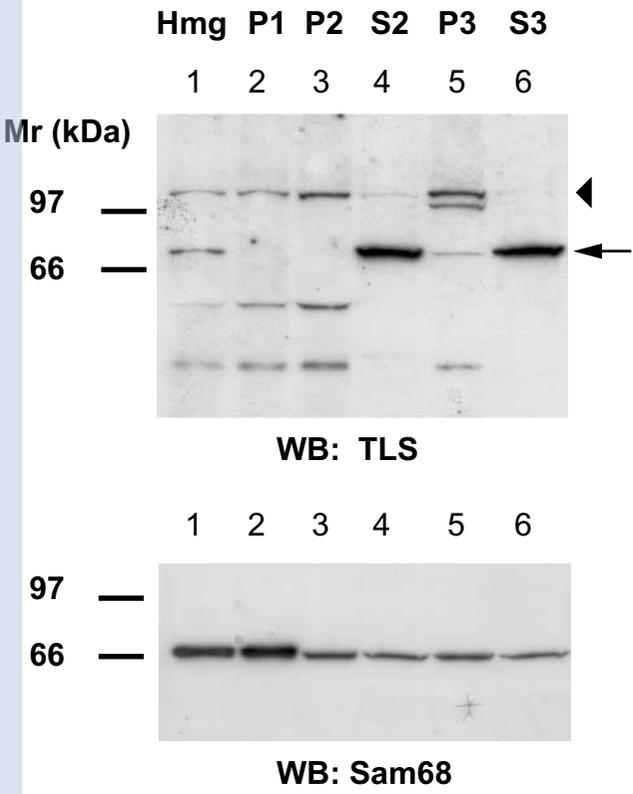
Figure

myc   TLS

HEK cells

A   B
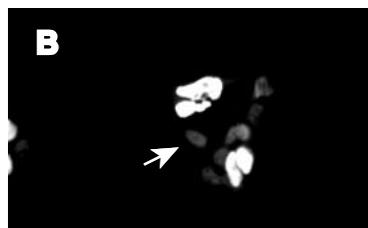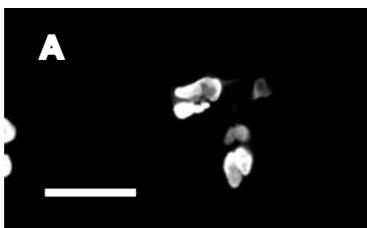
TLS   Sam68   Overlay

Dentate gyrus

C   s.mo.   D   E

Dentate gyrus

F   G   H

CA1

I   n   J   n   K

TLS   NR1   Overlay

CA1

L   M   N

TLS + GST

O

TLS + GST-TLS

P

Belly et al., Fig. 2

TLS **F-actin** **MAP2** **Overlay**

TLS **F-actin** **Overlay**